Characterization of normal breast tissue heterogeneity using time-resolved near-infrared spectroscopy.

Svensson, Tomas; Swartling, Johannes; Taroni, Paola; Torricelli, Alessandro; Lindblom, Pia; Ingvar, Christian; Andersson-Engels, Stefan

Published in:
Physics in Medicine and Biology

DOI:
10.1088/0031-9155/50/11/008

2005

Characterization of normal breast tissue heterogeneity using time-resolved near-infrared spectroscopy

2005 Phys. Med. Biol. 50 2559

(http://iopscience.iop.org/0031-9155/50/11/008)

INSTITUTE OF PHYSICS PUBLISHING PHYSICS IN MEDICINE AND BIOLOGY

Phys. Med. Biol. **50** (2005) 2559–2571 doi:10.1088/0031-9155/50/11/008

Characterization of normal breast tissue heterogeneity using time-resolved near-infrared spectroscopy

Tomas Svensson[1], Johannes Swartling[1], Paola Taroni[2], Alessandro Torricelli[2], Pia Lindblom[3], Christian Ingvar[3] and Stefan Andersson-Engels[1]

[1] Department of Physics, Lund Institute of Technology, Box 118, SE-221 00 Lund, Sweden
[2] Politecnico di Milano, Piazza Leonardo da Vinci 32, I-210 33 Milan, Italy
[3] Department of Surgery, Lund University Hospital, SE-221 85 Lund, Sweden

E-mail: tomas.svensson@fysik.lth.se, js604@cam.ac.uk, paola.taroni@polimi.it, alessandro.torricelli@polimi.it, pia.lindblom@skane.se, christian.ingvar@skane.se and stefan.andersson-engels@fysik.lth.se

Received 11 November 2004
Published 18 May 2005
Online at stacks.iop.org/PMB/50/2559

Abstract

In recent years, extensive efforts have been made in developing near-infrared optical techniques to be used in detection and diagnosis of breast cancer. Variations in optical properties of normal breast tissue set limits to the performance of such techniques and must therefore be thoroughly examined. In this paper, we present intra- and intersubject as well as contralateral variations of optical and physiological properties in breast tissue as measured by using four-wavelength time-resolved spectroscopy (at 660, 786, 916 and 974 nm). In total, 36 volunteers were examined at five regions at each breast. Optical properties (absorption, μ_a, and reduced scattering, μ_s') are derived by employing diffusion theory. The use of four wavelengths enables determination of main tissue chromophores (haemoglobin, water and lipids) as well as haemoglobin oxygenation. Variations in all evaluated properties seen over the entire breast are approximately twice those for small-scale heterogeneity (millimetre scale). Intrasubject variations in optical properties are almost in all cases below 20% for μ_s', and 40% for μ_a. Overall variations in water, lipid and haemoglobin concentrations are all in the order of 20%. Oxygenation is the least variable of the quantities evaluated, overall intrasubject variations being 6% on average. Extracted physiological properties confirm differences between pre- and post-menopausal breast tissue. Results do not indicate systematic differences between left and right breasts.

1. Introduction

The development of optical methods for detection and diagnosis of breast cancer has been pursued with increasing efforts during recent years. Optical methods for non-invasive tumour detection are based on near-infrared (NIR) light, typically within 600–1000 nm, which has the ability to propagate through tissue and yield a detectable reflected or transmitted signal. The NIR signal provides information on absorption and scattering properties of tissue, as well as spatial distribution of structures in the breast. The absorption coefficient μ_a and the reduced scattering coefficient μ_s' can be determined. This can be done locally, by using a probe based on a number of optical fibres to deliver and collect the light (Cubeddu *et al* 1999, Cerussi *et al* 2002, van Veen *et al* 2004a), or by imaging techniques such as diffuse optical tomography (Gratton *et al* 1993, Colak *et al* 1999, McBride *et al* 2001, Hebden *et al* 2002, Li *et al* 2003, Yates *et al* 2005) or by scanning the source and detector fibres across the compressed breast to record a shadowgram type image analogous to x-ray mammography (Franceschini *et al* 1997, Grosenick *et al* 2003, Taroni *et al* 2004). A key concept in these optical methods is the spectral information that can be derived if several wavelengths are used. Absorption properties can be used to quantify concentrations of chromophores in the tissue, of which the four principal ones are non-oxygen-saturated haemoglobin, oxygen-saturated haemoglobin, water and lipids (Sevick *et al* 1991, Matcher *et al* 1995, Cubbedu *et al* 1999). The spectral shape of the reduced scattering coefficient can provide valuable information about size and distribution of tissue scatterers, which in turn can be used to extrapolate structure and cellular composition of the tissue (Beauvoit *et al* 1994, Mourant *et al* 1997, Nilsson *et al* 1998, Cerussi *et al* 2001, Srinivasan *et al* 2003, Pifferi *et al* 2004).

Several investigations have been carried out to determine the relations between optical and physiological properties of normal breast tissue. Studies utilizing optical techniques have shown that breast tissue characteristics correlate with factors such as age (Cubeddu *et al* 1999, Cerussi *et al* 2001, Srinivasan *et al* 2003, Shah *et al* 2001), hormonal cycle (Cubeddu *et al* 2000), menopause status (Shah *et al* 2001, Cerussi *et al* 2002) and body mass index (Pogue *et al* 2001, Cerussi *et al* 2002, Durduran *et al* 2002). A number of investigators have also shown differences in the NIR signal for cancerous lesions as compared to normal tissue or benign lesions (Andersson-Engels 1992, Fantini *et al* 1998, Tromberg *et al* 2000, Pogue *et al* 2001, Grosenick *et al* 2003, Taroni *et al* 2004). These papers present a variability in optical properties for different lesions. Other studies have investigated the variability in optical properties of normal breast tissue (Shah *et al* 2004, van Veen *et al* 2004a, Pogue *et al* 2004). Of these, only Shah *et al* (2004) emphasize intrasubject variations. The overall variability implies an overlap between optical properties of lesions and normal tissue, which most likely precludes detection formulae based on direct analysis of absolute values of measured optical properties. Most certainly, detection methods will therefore be based on relative observations such as ratios, comparisons between different parts of the breast, comparisons between left and right breasts, or image contrast and context analysis in the case of imaging modalities. For this development, it is of fundamental importance to possess knowledge of the intrinsic variations of optical properties within a breast and between left and right breasts.

In this paper, we present an extensive investigation of intra- and intersubject heterogeneity in optical and physiological properties of normal breast tissue. A total number of 36 volunteers were included in the study. Optical properties were measured using four-wavelength time-resolved spectroscopy (Swartling *et al* 2003, Pifferi *et al* 2005) following a protocol comprising five measurement areas on each breast. Small-scale variations (millimetre displacements) were investigated thoroughly. A similar protocol was used by Shah *et al* (2004), in an investigation based on frequency-domain measurements at a fixed fibre separation.

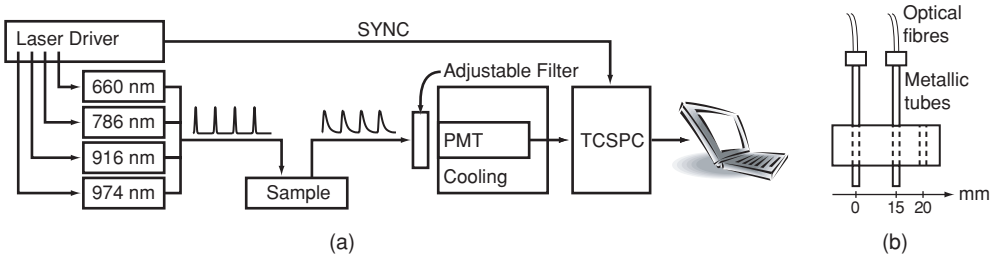

Figure 1. A schematic of the instrumentation in reflectance mode (a) and one of the probe while having 15 mm fibre separation (b).

In our study, most measurements were conducted using two different source and detector fibre separations, which means that different probing depths were used. This enables us to investigate spatial variation both laterally and axially.

2. Materials and methods

2.1. Instrumentation

All data were acquired using a compact and portable time-domain photon migration instrument primarily intended for spectroscopy of biological tissue in a clinical environment (Swartling *et al* 2003, Pifferi *et al* 2005). The system is based on diode laser technology and time correlated single photon counting (TCSPC). A laser driver (SEPIA PDL 808, PicoQuant, Germany) controls four pulsed diode lasers (LDH, PicoQuant at 660, 786, 916 and 974 nm). Wavelengths are chosen to enable monitoring of important tissue constituents (haemoglobin, water and lipids) and properties (tissue oxygenation). By separating the individual pulses in time (~ 6 ns), using electric cables of different lengths, it is possible to generate 4λ pulse trains at a repetition frequency up to 40 MHz. Diode lasers are coupled into 200 μm GRIN fibres (G 200/280 N, ART Photonics, Germany). A 4-1 coupler is used to couple all lasers into a 600 μm GRIN fibre (G 600/840 N, ART Photonics), which serves as the light source. A second 600 μm GRIN fibre collects light and delivers it to the detector. The length of these fibres were 1.95 m each. Since this work is based on diffuse reflectance measurements, these fibres were held by a probe that fixes them at a certain fibre separation (15 or 20 mm). The probe is made of a small metal block through which two metal tubes run (tubes may be moved to achieve proper separation). The metal tubes extend from the block, and optical fibres are inserted in these so that fibre endings are almost edge to edge with tube endings. The probe is held so that tube and fibre endings are in contact with the tissue. All parts are painted in mat black. Proper photon levels are achieved by sending collected light through an adjustable gradient ND filter. Remaining photons are sent into a cooled MCP-PMT (R3809-59, Hamamatsu Photonics, Japan). A TCSPC computer card (SPC-300, Becker & Hickl, Germany) is used to obtain time-dispersion curves. Lasers are typically operated at 1–2 mW generating pulses about 70 ps wide (FWHM). However, broadening in fibres and detector causes the instrument response function (IRF) to be about 100 ps wide. A schematic is given in figure 1.

2.2. Clinical procedure

Clinical data were collected at the Lund University Hospital adhering to a protocol approved by the local committee of ethics. Measurements were conducted during May and June 2003

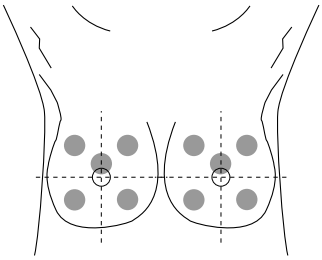

Figure 2. Location of measurement areas (five on each breast).

on in total 36 volunteers (29 pre-menopausal and 7 post-menopausal). Relevant medical information was collected in connection with the measurements. None of the volunteers had been diagnosed with malignant disease. All measurements were carried out while subjects were in a comfortable sitting posture. The probe was held by subjects themselves after careful instruction. Each breast was examined at five different areas: at the centre part of the four quadrants and just above the areolar area (denoted left/right (L/R) upper outer (UO), upper inner (UI), lower inner (LI), lower outer (LO) and upper areolar (UA)). Locations of measurement areas are illustrated in figure 2. Six out of the thirty-six volunteers were examined using only the 20 mm fibre separation, and following a more comprehensive protocol P1 where (i) five spatially separated measurements are performed within each area (small millimetre-scale probe displacements) and (ii) five spatially identical measurements (fixed probe geometry) are performed at the upper outer areas (RUO and LUO) to ensure/monitor stability. The remaining 30 volunteers were examined using two different fibre separations (15 and 20 mm) and a different protocol P2. In these cases each area was only measured once, except for the upper outer areas which were measured three times (spatially separated in the case of ROU and spatially identical in the case of LOU). Typically, a single measurement was completed within 20–30 s.

2.3. Modelling

Experimental data are modelled using the diffusion approximation of transport theory. The particular model used in this work is derived for the case of homogenous media in a semi-infinite geometry and employs a so-called extrapolated boundary condition (Haskell *et al* 1994, Hielscher *et al* 1995). The refractive index of tissue is assumed to be 1.4. Tissue optical properties are extracted by fitting solutions of the diffusion equation to experimental data. An example on how data may appear is given in figure 3. To avoid problems related to early photons, such as poor validity of the diffusion equation and stray light, fitting is limited to datapoints where the photon count exceeds 30% of the peak count on the rising flank (see figure 3). The trailing flank is cut where the photon count drops below 1% of the peak count. Discussions on appropriate fit regions are found in Hielscher *et al* (1995) and Cubeddu *et al* (1996). The best fit is reached iteratively using a Levenberg–Marquardt algorithm, where μ_s', μ_a and an overall amplitude (scale) factor are varied in order to minimize the χ^2 error norm. The temporal delay between IRF and experimental data is known and is thus not a free parameter. Each iteration involves a convolution between the theoretical time-dispersion curve and the IRF. The IRF is carefully measured before and after every set of measurements to ensure stability and, as mentioned above, since it is needed in data evaluation.

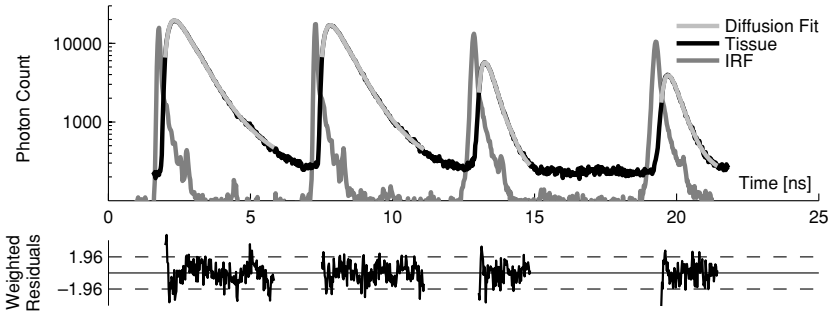

Figure 3. Example of time-resolved data. The 4λ pulsetrains correspond to (from left to right) 660, 786, 916 and 974 nm. Experimental curves (tissue) are partially hidden behind fitted diffusion curves, indicating reasonable fits. Residuals occasionally and non-systematically exhibit non-random patterns (as seen for 660 nm in this example). [−1.96, 1.96] is a 95% prediction interval for a standardized normal distribution.

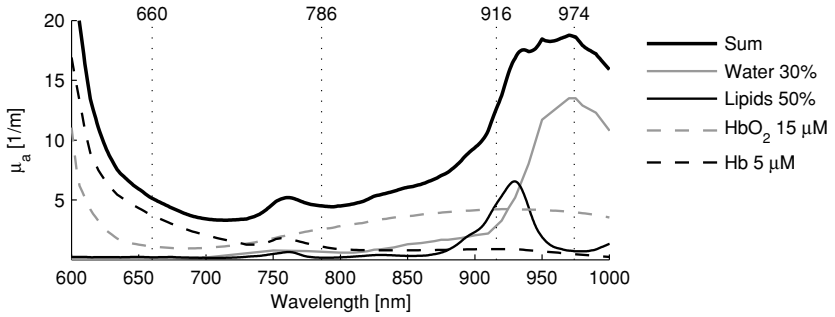

Figure 4. A typical breast tissue spectrum constructed from component spectra. Vertical dotted lines mark where diode lasers are positioned. Note that oxy-haemoglobin, lipid and water absorption exhibit comparable strengths in the range 900–950 nm.

Tissue constituents are determined using the four extracted absorption coefficients. The use of four wavelengths enables calculations of concentration for the four main chromophores in breast tissue: water, lipids, deoxy-haemoglobin (Hb) and oxy-haemoglobin (HbO_2). The assumption is that the observed absorption match a linear superposition of the four main component spectra, and that no other tissue constituents contribute to the absorption in this wavelength region. The haemoglobin spectra are taken from Prahl (2004), the water spectrum from Hale and Querry (1973) and the lipid spectrum from van Veen *et al* (2004b). An example of an interpreted breast spectrum composed of the four tissue chromophores in typical concentrations is shown in figure 4. Mathematically, concentrations are calculated by solving a set of linear equations

$$\boldsymbol{\mu}_a = \boldsymbol{A} \cdot \boldsymbol{c} \quad \Rightarrow \quad \boldsymbol{c} = \boldsymbol{A}^{-1} \cdot \boldsymbol{\mu}_a \tag{1}$$

where $\boldsymbol{\mu}_a$ is a vector of extracted absorption coefficients at the four wavelengths, $\boldsymbol{A}$ a matrix of absorption coefficients for the four chromophores at the four wavelengths measured and $\boldsymbol{c}$ a vector of concentrations. Haemoglobin concentrations [Hb] and [HbO_2] are measured in μM, while water and lipid concentrations are measured in volume per cent (per cent relative to pure water and lipid, respectively). Oxygenation (S_tO_2) is determined by the ratio of [HbO_2] to total haemoglobin concentration [Hb] + [HbO_2] (THC). Error propagation is discussed in section 4.

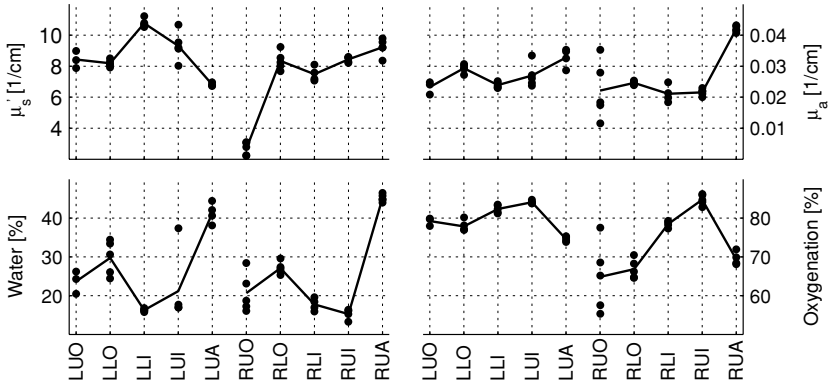

Figure 5. Derived optical (660 nm) and physiological parameters grouped by position, originating from one volunteer (age 33 years) examined according to protocol P1. In this particular case, extremely low scattering is extracted at one position (RUO). Markers correspond to extracted values within series of small-scale probe displacements. Lines join positional averages. Data from the left and right breasts are presented separately in each graph.

Table 1. Positional averages of optical and physiological properties (this study). Results are compared with values from recent literature. N states the number of subjects involved in the different studies. Optical properties, μ_s' and μ_a, are extracted at 785 or 786 nm.

	N	μ_s' (cm^{-1})	μ_a (cm^{-1})	THC (μM)	Oxygenation (%)
This study	36	8.0 ± 2.0	0.041 ± 0.021	17 ± 10	77 ± 8
Spinelli *et al* (2004)	>50	11.3 ± 2.1	0.037 ± 0.013	16 ± 5	66 ± 9
Grosenick *et al* (2003)	28	10.2 ± 1.6	0.039 ± 0.009	17 ± 8	74 ± 3
Durduran *et al* (2002)	52	8.5 ± 2.1	0.041 ± 0.025	34 ± 9	68 ± 8

2.4. Variational measures

Intrasubject variations are characterized using coefficients of variation (CV). The CV of a certain series $\{x_i\}$ is defined as the standard deviation divided by the mean: $\mathrm{CV}_x = \sigma_x/\overline{x}$. It is a unitless quantity stated in per cent.

The CV of a fixed geometry series states the variations induced mainly by instrumentation and measurement parameters, such as e.g. probe-skin pressure, as well as noise in the signal. The CV of a displacement series is a measure of the local intrasubject variation within different measurement areas. Overall intrasubject variation is, in this work, defined as the CV of the ten average values obtained for the ten different positions.

3. Results

An example of how extracted data may appear is given in figure 5. Here, a selection of data from one volunteer examined according to protocol P1 is presented. Average properties, based on all volunteers, are presented and compared to values from literature in table 1.

A statistical analysis of intrasubject variations for fixed geometries (F), small-scale displacements (D) and overall (O) is shown in figure 6. Variations in fixed geometry series are typically very small compared to variations in series where the probe is displaced, as long as the probe is held properly (no change in pressure or orientation). However, if probe-skin pressure or probe orientation is varied (still using a fixed position) variations

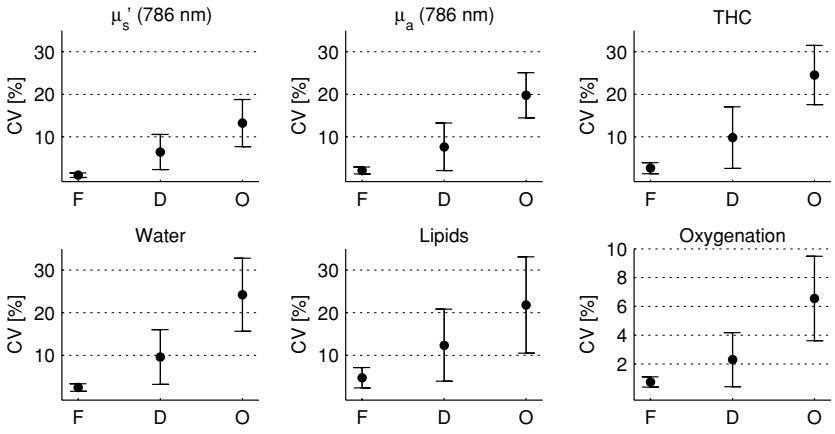

Figure 6. Intrasubject variation in fixed series (F, $m = 42$), displacement series (D, $m = 90$) and overall (O, $m = 36$), where m follows from study protocols and refers to the number of underlying series. Variations are given in CV (%). Dots represent the average intrasubject CV and error bars stretch out to $\pm\sigma$, where σ is the standard deviation of the CV distribution. Data are based on series from $n = 36$ volunteers.

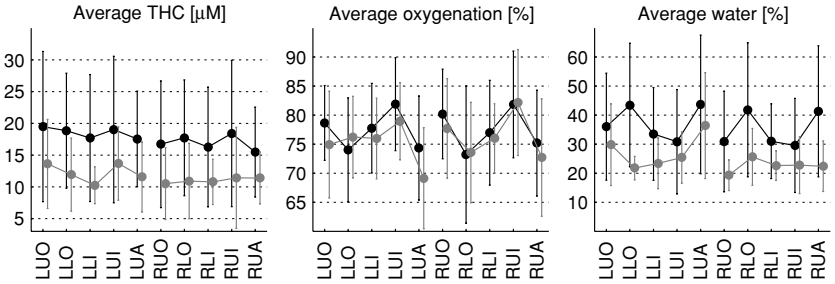

Figure 7. Average values versus measurement position. Volunteers are divided in two groups: pre-menopausal ($n = 29$, black) and post-menopausal ($n = 7$, grey). 20 mm fibre separation.

occasionally are in the same order. Derived optical and physiological properties indicate that the overall intrasubject variation is typically a factor of 2 greater than variations within displacement series (a factor of 4 in the case of S_tO_2). Overall intrasubject variations in μ_s' were $(14.0 \pm 6.5)\%$, $(13.2 \pm 5.6)\%$, $(15.1 \pm 5.5)\%$ and $(15.3 \pm 6.0)\%$, for 660, 786, 916 and 974 nm respectively. μ_a varied even more, and corresponding figures were $(23.1 \pm 8.3)\%$, $(19.8 \pm 5.3)\%$, $(11.8 \pm 3.6)\%$ and $(20.4 \pm 8.3)\%$ (the largest variation was 48.7% and was registered at 974 nm, but CVs above 40% were very rare). S_tO_2 displays the smallest overall intrasubject variation, being $(6.6 \pm 2.9)\%$ (in all cases below 14.2%).

In order to better understand these variations, the data were analysed to provide intersubject variation with respect to positional averages. Figure 7 shows the result for haemoglobin, oxygenation and water. In these graphs, pre-menopausal and post-menopausal volunteers are considered as two separate groups. Concentrations of haemoglobin and water were both approximately 1.5 times greater, on average, for pre-menopausal volunteers. On the other hand, lipid concentration was approximately 1.4 times greater for post-menopausal volunteers. Nonetheless, variations within the two groups cause overlap. No significant differences were noted neither for oxygenation levels or scattering levels (not shown).

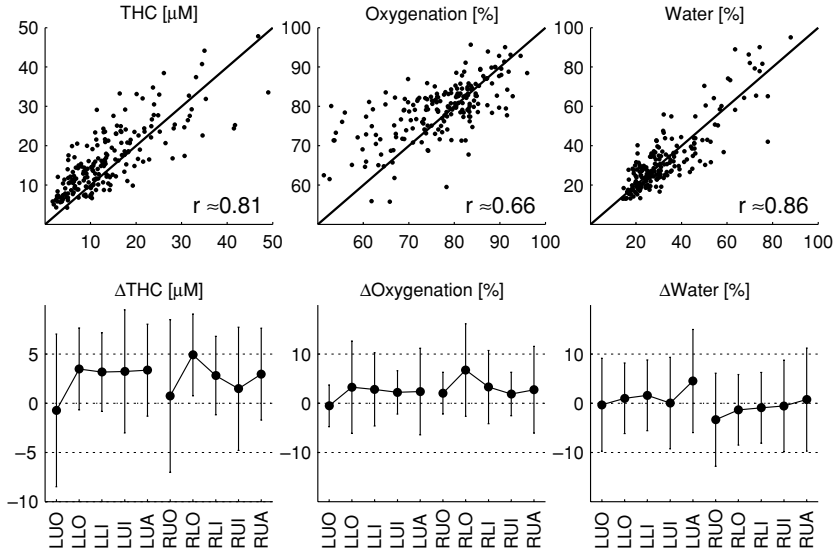

Figure 8. Upper row: scatter plots showing correlation between results obtained using different fibre separations (15 mm (x axis) and 20 mm (y axis)). Correlation coefficient r and diagonals are added for reference. Lower row: average difference, $\Delta = \Delta_{20-15}$, grouped on measurement position. Error bars stretch out to $\pm\sigma$.

By changing the separation between probe fibres, the influence of probing depth was examined. Correlations between data obtained for the two fibre separations are stated using the correlation coefficient r. Fairly strong correlations between the two ways of measuring were observed for all optical and physiological properties. Lowest correlation was found in scattering (on average $r = 0.51$). Correlations (r) were on average 0.78 for absorption, 0.67 for lipids and 0.86 for water. No significant differences were observed in the cases of lipids, water or scattering. However, as indicated in figure 8, extracted levels of oxygenation and haemoglobin tended to be systematically higher when using the larger fibre separation (20 mm).

Intrasubject variations between left and right breasts were examined by comparing corresponding measurements. The result does not indicate any significant systematic differences. Left–right asymmetry in a certain parameter p is measured using relative deviation Δ_{rel}

$$\Delta_{\text{rel}} = \frac{|p_{\text{left}} - p_{\text{right}}|}{(p_{\text{left}} + p_{\text{right}})/2} \tag{2}$$

where p_{left} and p_{right} are (mean) values derived at a certain measurement area. Δ_{rel} is a unitless quantity that states the deviation in % of the mean of the left and right parameter values. Results are presented in table 2.

4. Discussion

The main purpose of this study is to measure variations in tissue composition of normal breasts and discuss how such variations may influence the possibility of discriminating a possible tumour using optical methods. Nevertheless, it is important to note that fundamental optical and physiological properties derived in this study are in good agreement with previously

Table 2. Variations between the left and right breasts stated in relative deviation Δ_{rel} (% of mean). Values presented are means of the individual relative left–right deviation derived for all $n = 36$ volunteers (20 mm fibre separation).

	UO	LO	LI	UI	UA
THC	27	19	19	26	26
Oxygenation	6	8	5	5	9
Water	28	15	17	19	24
Lipid	24	36	20	22	26
Scattering (786 nm)	11	12	13	15	15

published data (see table 1). Deviations may be assigned to differences in measurement geometry. The statistical analysis of spatial variations within breast tissue, as measured in this study, is illustrated in figure 6. On average, variations once the probe was held fixed in the same position are small for all properties evaluated. Variations in these measurements are not believed to reflect any changes within the tissue structure, but rather variations in how the probe was applied to the tissue, mainly due to pressure variations, as well as uncertainties in the evaluation of the signals due to noise. As soon as the probe was displaced a few millimetres to include small-scale tissue variability, variations increased for all parameters. Interestingly, water, lipid and haemoglobin concentrations varied considerably more (a factor 5) than the oxygenation (as also reported by Shah *et al* (2004)). Variations in evaluated constituent concentrations are believed to be due to the heterogeneous structure of breast tissue even at this small scale (millimetres). The oxygenation of haemoglobin present in the probe volume is, however, less likely to alter for these small displacements. Oxygenation is high everywhere in normal breasts.

Variations in all evaluated properties seen over the entire breast are approximately twice those registered for small-scale displacements of the probe. The increased variability for these measurements can, at least partly, be explained by more systematic alterations in tissue structure and composition at different parts of the breast. Such variations are presented in figure 7. In general, strong overlaps exist between values for different locations. However, while total haemoglobin concentration is relatively even throughout the breast, oxygenation seems to be slightly higher in the upper inner area of the breast and lower in the upper areolar area. Shah *et al* (2004) report significantly lower oxygenation in areolar regions, but no significant variations among other regions. Worth noting is also that intrasubject variations in μ_a is a factor 2 smaller at 916 nm than at the other three wavelengths. This is related to the fact that lipids and water exhibit comparable absorption strengths in this region, and that these two constituents, to a large extent, replace each other (Pifferi *et al* 2004, Swartling *et al* 2005).

The data also show differences in total haemoglobin and water concentrations for pre- and post-menopausal women. Such changes are in accordance with known structural alterations of breast tissue after menopause (Shah *et al* 2004). However, one should also have in mind that there is a difference in age between the two groups. The mean ages for the two groups in this study are 37 and 52 years, respectively. In the material, it is also evident that the composition of the breast may be quite different in different persons. Intersubject variations are thus much higher than intrasubject variations (see figure 7).

Heterogeneity of breast tissue has previously been addressed by Shah *et al* (2004). Their investigation presents small-scale variations in the same order as our report. Overall heterogeneity is similar in the case of water, lipids, THC and oxygenation. However, Shah *et al* (2004) report on an overall heterogeneity less than 12% for μ_s' while we observe corresponding values up to approximately 20%. The generally good agreement in results was obtained despite

differences in measurement technique (time-domain versus frequency-domain), measurement geometry (probe design, sitting versus supine position) and possibly also in exact measurement positions.

By using two different distances between the source and detector fibres we probe different depths of the tissue (Patterson *et al* 1995). For time-resolved data the probing depth is also a function of the time the light has spent in the tissue. The evaluation of μ_s' in the fitting process is sensitive to the early portion of the light, while μ_a is mostly determined by the late light (Andersson-Engels *et al* 1992, Cubeddu *et al* 1996). This means that the extracted values of μ_s' and μ_a do not represent the exact same volume, even for the same fibre separation. Scattering values represent a shallow volume confined to the region between the two fibres, while the absorption values are derived from a larger volume deeper in the tissue. When performing measurements, for practical reasons, the probe had to be lifted between the measurements at 15 mm and 20 mm fibre separation. Repositioning of the probe could not be done with better accuracy than a few millimetres, which means that we can expect a random variation in the results of at least the same order of magnitude as that given by small displacements of the probe, as shown in figure 6. This is seen in the scatter plots in figure 8. The difference in effective probing volume for determination of μ_a and μ_s' may explain the lower degree of correlation for μ_s' ($r = 0.51$) compared to μ_a ($r = 0.78$). Moreover, we noted an average increase in both THC and S_tO_2 when increasing the fibre separation from 15 mm to 20 mm, as seen in figure 8. This may be interpreted as a higher haemoglobin concentration and oxygen saturation at larger depth, and is in agreement with the known structure of tissue: at short fibre separations, the probing volume is more affected by the skin layer, which has lower blood perfusion. Similar findings were reported by Pifferi *et al* (2004), where the fibre separation was increased from 20 to 40 mm.

All data presented in this study are based on rather superficial measurements on breasts, including skin, subcutaneous fat and breast tissue. This will often be the case in diagnostic procedures based on non-invasive optical spectroscopy. Due to the aim to measure local properties in the same spatial scale as would be of interest for tumour diagnostics, without relying on a tomographic algorithm, the interfibre distance is short. This results in a relatively large fraction of the probed tissue being occupied by subcutaneous fat, especially for women with high body mass index (BMI). Unfortunately, the material is not sufficiently large to make a correlation with BMI. However, Pifferi *et al* (2004) report that the kind of diffuse reflectance measurements employed in this paper provide representative values even for interior breast tissue. Whether this also hold for interior heterogeneity is unclear and is currently examined both in Lund and elsewhere.

In this work, breast spectra are sampled at four wavelengths. Since equally many (four) chromophores need to be taken into account, it is very important that all of the four derived absorption coefficients are accurate. According to basic perturbation theory, errors in $\boldsymbol{c}$ (denoted $\delta\boldsymbol{c}$) are related to errors in $\boldsymbol{\mu}_a$ (denoted $\delta\boldsymbol{\mu}_a$) as shown in (3).

$$\boldsymbol{c} = \boldsymbol{c}^{\text{true}} + \delta\boldsymbol{c} = \boldsymbol{A}^{-1} \cdot \left(\boldsymbol{\mu}_a^{\text{true}} + \delta\boldsymbol{\mu}_a\right) \quad \Rightarrow \quad \delta\boldsymbol{c} = \boldsymbol{A}^{-1} \cdot \delta\boldsymbol{\mu}_a. \tag{3}$$

Thus, influence of errors in extracted absorption coefficients may be examined by taking a closer look at the matrix $\boldsymbol{A}^{-1}$. Relative errors naturally depend on the tissue constitution of the particular breast (i.e. $\boldsymbol{c}^{\text{true}}$ and $\boldsymbol{\mu}_a^{\text{true}}$). By proper normalization of $\boldsymbol{A}^{-1}$ it is possible to determine a relative error propagation matrix, $\boldsymbol{E}$, that states component-wise relative error propagation (valid for a particular tissue composition). The normalization procedure is defined in 4, where $\text{diag}(\cdots)$ are diagonal 4×4 matrices.

$$\boldsymbol{E} = \boldsymbol{E}\left(\boldsymbol{A}^{-1}, \boldsymbol{c}^{\text{true}}, \boldsymbol{\mu}_a^{\text{true}}\right) = \text{diag}(1/\boldsymbol{c}^{\text{true}}) \cdot \boldsymbol{A}^{-1} \cdot \text{diag}\left(\boldsymbol{\mu}_a^{\text{true}}\right). \tag{4}$$

When considering breast tissue having the composition as shown in figure 4 one finds that

$$\boldsymbol{E} = \begin{pmatrix} 1.58 & -0.56 & -0.12 & 0.11 \\ -0.74 & 2.27 & -0.12 & -0.41 \\ 0.27 & -1.59 & 2.90 & -0.58 \\ 0.15 & -0.56 & -0.11 & 1.53 \end{pmatrix}. \tag{5}$$

Here, each column corresponds to a certain wavelength (660, 786, 916 and 974 nm, from left to right) and each row to a certain chromophore (Hb, HbO_2, lipids and water, from top to bottom). As an example, a + 1% error in μ_a at 786 nm will add a +2.27% error on HbO_2 concentration (when measuring on a tissue consisting of 50% lipids, 30% water, 5 μM Hb and 15 μM HbO_2). $\boldsymbol{E}$ gives an idea of the robustness of four-wavelength spectroscopy when applied to characterization of breast tissue. The diagonal dominance implies that each chromophore has its own main wavelength (this is also seen in figure 4). The relatively large numbers in the third row show that the derivation of lipid concentrations suffer the greatest sensitivity to errors. This is due to that lipid absorption normally does not dominate over other chromophores at any wavelength (this is exemplified in the breast spectra presented in figure 4). This is a possible explanation to why lipid levels, in comparison with other chromophore levels, exhibit larger variations within fixed series (see figure 6).

5. Conclusion

In summary, we have investigated the influence of normal spatial heterogeneities of breast tissue on optical and related physiological properties measured with a four-wavelength, time-resolved diffuse spectroscopy instrument. Variations in evaluated properties over all measurement areas were about twice as large as small-scale variations (mm displacements). Intrasubject variation was in almost all cases below 40% for μ_a and below 20% for μ_s'. In terms of the evaluated quantities of water, lipids and haemoglobin, the variation in these were all in the order of 20%, while the oxygen saturation exhibited a lower variation (6%). These numbers define a background variation that any modality for optical detection of breast cancer has to take into account. Furthermore, we did not see any evidence of systematic differences between contralateral breasts, although individual left–right asymmetry is often seen. The intersubject variation is larger than the intrasubject variation and is loosely correlated with menopause status, which confirms previous studies. Finally, measurements performed at different fibre separations, thus probing different depths, indicated an on average higher haemoglobin concentration at the larger fibre separation. Random variations were in this case comparable to those seen for small-scale displacements.

Acknowledgments

This work was financially supported by OPTIMAMM (European grant QLG1-2000-00690), MEDPHOT (European grant QLG1-2000-01464), CUSBO (European grant HPRI-CT-2001-00148) as well as the Swedish Research Council. The authors also wish to thank all volunteers for their participation.

References

Andersson-Engels S, Berg R and Svanberg S 1992 Effects of optical constants on time-gated transillumination of tissue and tissue-like media *J. Photochem. Photobiol.* B **16** 155–67

Beauvoit B, Kitai T and Chance B 1994 Contribution of the mitochondrial compartment to the optical properties of the rat liver: a theoretical and practical approach *Biophys. J.* **67** 2501–10

Cerussi A, Berger A J, Bevilacqua F, Shah N, Jakubowski D, Butler J, Holocombe R F and Tromberg B J 2001 Sources of absorption and scattering contrast for near-infrared optical mammography *Acta Radiol.* **8** 211–8

Cerussi A E, Jakubowski D, Shah N, Bevilacqua F, Lanning R, Berger A J, Hsiang D, Butler J, Holcombe R F and Tromberg B J 2002 Spectroscopy enhances the information content of optical mammography *J. Biomed. Opt.* **7** 60–71

Colak S B, van der Mark M B, 't Hooft G W, Hoogenraad J H, van der Linden E S and Kuijpers F A 1999 Clinical optical tomography and NIR spectroscopy for breast cancer detection *IEEE J. Sel. Top. Quantum Electron.* **5** 1143–58

Cubeddu R, D'Andrea C, Pifferi A, Taroni P, Torricelli A and Valentini G 2000 Effects of the menstrual cycle on the red and near-infrared optical properties of the human breast *Photochem. Photobiol.* **72** 383–91

Cubeddu R, Pifferi A, Taroni P, Torricelli A and Valentini G 1996 Experimental test of theoretical models for time-resolved reflectance *Med. Phys.* **23** 1625–33

Cubeddu R, Pifferi A, Taroni P, Torricelli A and Valentini G 1999 Noninvasive absorption and scattering spectroscopy of bulk diffusive media: an application to the optical characterization of human breast *Appl. Phys. Lett.* **74** 874–6

Durduran T, Choe R, Culver J P, Zubkov L, Holboke M J, Giammarco J, Chance B and Yodh A G 2002 Bulk optical properties of healthy female breast tissue *Phys. Med. Biol.* **47** 2847–61

Fantini S, Walker S A, Franceschini M A, Kaschke M, Schlag P M and Moesta K T 1998 Assessment of the size, position, and optical properties of breast tumors *in vivo* by noninvasive optical methods *Appl. Opt.* **37** 1982–9

Franceschini M A, Moesta K T, Fantini S, Gaida G, Gratton E, Jess H, Mantulin W W, Seeber M, Schlag P M and Kaschke M 1997 Frequency-domain techniques enhance optical mammography: initial clinical results *Proc. Natl. Acad. Sci. USA* **94** 6468–73

Gratton E, Mantulin W W, vandeVen M J, Fishkin J, Maris M B and Chance B 1993 A novel approach to laser tomography *Bioimaging* **1** 40–6

Grosenick D, Moesta K T, Wabnitz H, Mucke J, Stroszczynski C, Macdonald R, Schlag P M and Rinneberg H 2003 Time-domain optical mammography: initial clinical results on detection and characterization of breast tumors *Appl. Opt.* **42** 3170–86

Hale G M and Quearry M R 1973 Optical constants of water in the 200-nm to 200-μm wavelength region *Appl. Opt.* **12** 555–63

Haskell R C, Svaasand L O, Tsay T-T, Feng T-C, McAdams M S and Tromberg B J 1994 Boundary conditions for the diffusion equation in radiative transfer *J. Opt. Soc. Am.* A **11** 2727–41

Hebden J C, Bland T, Hillman E M C, Gibson A, Everdell N and Delpy D 2002 Optical tomography of the breast using a 32-channel time-resolved imager *OSA Biomedical Topical Meetings, OSA Technical Digest* pp 187–9

Hielscher A H, Jacques S L, Wang L H and Tittel F K 1995 The influence of boundary-conditions on the accuracy of diffusion-theory in time-resolved reflectance spectroscopy of biological tissues *Phys. Med. Biol.* **40** 1957–75

Li A *et al* 2003 Tomographic optical breast imaging guided by three-dimensional mammography *Appl. Opt.* **42** 5181–90

Matcher S J, Elwell C E, Cooper C E, Cope M and Delpy D T 1995 Performance comparison of several published tissue near-infrared spectroscopy algorithms *Anal. Biochem.* **227** 54–68

McBride T O, Pogue B W, Jiang S, Osterberg U L and Paulsen K D 2001 A parallel-detection frequency-domain near-infrared tomography system for hemoglobin imaging of the breast *in vivo Rev. Sci. Instrum.* **72** 1817–24

Mourant J R, Fuselier T, Boyer J, Johnson T M and Bigio I J 1997 Predictions and measurements of scattering and absorption over broad wavelength ranges in tissue phantoms *Appl. Opt.* **36** 949–57

Nilsson A M K, Sturesson C, Liu D L and Andersson-Engels S 1998 Changes in spectral shape of tissue optical properties in conjunction with laser-induced thermotherapy *Appl. Opt.* **37** 1256–67

Patterson M S, Andersson-Engels S, Wilson B C and Osei E K 1995 Absorption spectroscopy in tissue-simulating materials: a theoretical and experimental study of photon paths *Appl. Opt.* **34** 22–30

Pifferi A *et al* 2005 Performance assessment of photon migration instruments: the MedPhot protocol *Appl. Opt.* accepted

Pifferi A, Swartling J, Chikoidze E, Torricelli A, Taroni P, Bassi A, Andersson-Engels S and Cubeddu R 2004 Spectroscopic time-resolved diffuse reflectance and transmittance measurements of the female breast at different interfiber distances *J. Biomed. Opt.* **9** 1143–51

Pogue B W, Jiang S D, Dehghani H, Kogel C, Soho S, Srinivasan S, Song X M, Tosteson T D, Poplack S P and Paulsen K D 2004 Characterization of hemoglobin, water, and NIR scattering in breast tissue: analysis of intersubject variability and menstrual cycle changes *J. Biomed. Opt.* **9** 541–52

Pogue B W, Poplack S P, McBride T O, Wells W A, Osterman K S, Osterberg U L and Paulsen K D 2001 Quantitative hemoglobin tomography with diffuse near-infrared spectroscopy: pilot results in the breast *Radiology* **218** 261–6

Prahl S A 2004 http://omlc.ogi.edu/spectra/hemoglobin/summary.html

Sevick E M, Chance B, Leigh J, Nioka S and Maris M 1991 Quantitation of time- and frequency-resolved optical spectra for determination of tissue oxygenation *Anal. Biochem.* **195** 330–51

Shah N, Cerussi A, Eker C, Espinoza J, Butler J, Fishkin J, Hornung R and Tromberg B 2001 Noninvasive functional optical spectroscopy of human breast tissue *Proc. Natl Acad. Sci. USA* **98** 4420–5

Shah N, Cerussi A E, Jakubowski D, Hsiang D, Butler J and Tromberg B J 2004 Spatial variations in optical and, physiological properties of healthy breast tissue *J. Biomed. Opt.* **9** 534–40

Spinelli L, Torricelli A, Pifferi A, Taroni P, Danesini G M and Cubeddu R 2004 Bulk optical properties and tissue components in the female breast from multiwavelength time-resolved optical mammography *J. Biomed. Opt.* **9** 1137–42

Srinivasan S, Pogue B W, Jiang S D, Dehghani H, Kogel C, Soho S, Gibson J J, Tosteson T D, Poplack S P and Paulsen K D 2003 Interpreting hemoglobin and water concentration, oxygen saturation, and scattering measured *in vivo* by near-infrared breast tomography *Proc. Natl Acad. Sci. USA* **100** 12349–54

Swartling J, Pifferi A, Giambattistelli E, Chikoidze E, Torricelli A, Taroni P, Andersson M, Nilsson A and Andersson-Engels S 2003 Rigorous characterization of time-resolved diffuse spectroscopy systems for measurements of absorption and scattering properties using solid phantoms *Proc. SPIE* **5138** 80–7

Swartling J, Svensson J, Bengtsson D, Terike K and Andersson-Engels S 2005 Fluorescence spectra provide information on the depth of fluorescent lesions in tissue *Appl. Opt.* **44** 1934–41

Taroni P, Danesini G, Torricelli A, Pifferi A, Spinelli L and Cubeddu R 2004 Clinical trial of time-resolved scanning optical mammography at 4 wavelengths between 683 and 975 nm *J. Biomed. Opt.* **9** 464–73

Tromberg B J, Shah N, Lanning R, Cerussi A, Espinoza J, Pham T, Svaasand L O and Butler J 2000 Non-invasive *in vivo* characterization of breast tumors using photon migration spectroscopy *Neoplasia* **2** 26–40

van Veen R L P, Sterenborg H J C M, Marinelli A W K S and Menke-Pluymers M 2004a Intraoperatively assessed optical properties of malignant and healthy breast tissue used to determine the optimum wavelength of contrast for optical mammography *J. Biomed. Opt.* **9** 1129–36

van Veen R L P, Sterenborg H J C M, Pifferi A, Torricelli A and Cubeddu R 2004b Determination of VIS-NIR absorption coefficients of mammalian fat, with time- and spatially resolved diffuse reflectance and transmission spectroscopy *Biomedical Topical Meetings* (Washington: Optical Society of America)

Yates T D, Hebden J C, Gibson A P, Everdell N L, Arridge S R and Douek M 2005 Optical tomography of the breast using a multi-channel time-resolved imager *Phys. Med. Biol.* **50** 2503–17